JOURNAL OF AIRCRAFT
Vol. 31, No. 1, Jan.–Feb. 1994

Suppression of Flow-Induced Pressure Oscillations in Cavities

R. L. Sarno* and M. E. Franke†
Air Force Institute of Technology, Wright-Patterson Air Force Base, Ohio 45433

Experimental methods for suppressing flow-induced pressure oscillations in a shallow cavity resulting from tangential flows over the cavity are described. The effects of manipulating the shear layer over the cavity leading edge are examined. Static and oscillating fences and steady and pulsating flow injection at the leading edge are studied for their effect on cavity sound pressure levels. Both subsonic and supersonic flow conditions are considered. Of the methods tested, static fences at the leading edge were found to provide the most suppression. Suppression was dependent on the frequency mode and the flow Mach number.

Nomenclature

a = speed of sound
D = cavity depth
f = frequency
k = vortex convection velocity to freestream velocity ratio
L = cavity length
M = Mach number
m = frequency mode number
P = pressure
P_0 = stagnation pressure
Re = Reynolds number, Ux/ν
S = Strouhal number
S^* = modified Strouhal number
U = freestream velocity
x = distance from nozzle exit
Z = cavity span, lateral dimension
α = phase delay parameter
γ = ratio of specific heats
δ = boundary-layer thickness
ν = kinematic viscosity

Introduction

AIR flowing tangentially over a cavity in a surface can induce pressure oscillations within the cavity. In many cases these oscillations are large enough to cause adverse effects on the cavity and the items within the cavity. For example, in an aircraft weapon bay, oscillations can affect the structural integrity of the cavity, cause store restraint and release mechanisms to fail, damage sensitive stores, and affect store separation from the aircraft. Oscillations may also adversely affect the avionics on board.

Over the past 35 yr, there have been numerous investigations of flows over cavities. A recent survey of flows over cavities by Komerath et al.[1] included, among other things, classifications of cavity flows, observed phenomena, prediction methods, suppression techniques, and an extensive bibliography. Other reviews of cavity flows include those by Rockwell[2] and Rockwell and Naudascher.[3] Early studies by Karamcheti[4] showed that the intensities of the pressure oscillations were higher when the boundary layer upstream of the cavity was laminar rather than turbulent. Following this article,[4] interest in cavity flow-induced pressure oscillations and their control has continued. A number of other studies[5–12] are of particular interest. For example, Heller and Bliss[5,6] conducted research related to the physical mechanisms and suppression techniques of flow-induced pressure fluctuations in cavities.

Cavities with a length-to-depth ratio greater than one are generally referred to as shallow cavities.[1] Flows over these cavities cause flow-induced oscillations that result from the interaction of the free shear layer and the medium within the cavity.[5] Furthermore, Heller and Bliss[5,6] indicated that the unsteady motion of the shear layer above the cavity results in mass addition and removal at the cavity trailing edge. In shallow cavities this mass addition and removal process is similar to that of a cavity whose rear bulkhead acts like an oscillating piston. Open cavities are those where the shear layer attaches at or downstream of the back wall, whereas in closed cavities the shear layer may attach to the cavity floor.[1]

Studies have shown that pressure oscillation amplitudes can be reduced if the shear layer over the cavity can be stabilized to prevent the mass addition and removal process at the cavity trailing edge. Several passive-type methods[5–7] of stabilizing the shear layer, such as the use of fences and ramps, have achieved modest results, although the effectiveness of any particular suppression device is usually Mach number dependent.[7] Sarohia and Massier[8] found that mass injection at the base of the cavity suppressed cavity flow noise. Since it has been shown that the cavity pressure oscillations tend to occur at discrete frequencies for a given flow condition, perhaps the shear layer could be forced at a frequency different from the resonant frequencies, or at some submultiple of the resonant frequency with a phase change to reduce the pressure oscillation amplitudes. Forcing of the shear layer might be accomplished by various mechanical, acoustical, or fluid injection methods.

The purpose of this experimental investigation was to determine the effectiveness of suppressing pressure oscillations by manipulating the shear layer of high-speed tangential flow over a rectangular cavity that is shallow ($L/D = 2$) and narrow ($L/Z = 6.4$). In this type of cavity the response is primarily two-dimensional, and the freestream flow direction dominates the internal cavity flow so that three-dimensional effects are restricted to small perturbations in the dominant flow direction within the cavity.[5,9] However, three-dimensional effects in the flowfield may be considerable, and are not accounted for in this study since the side walls of the cavity also form the side walls of the flowfield over the cavity. The shallow cavities in this study are considered open cavities. Suppression techniques included a static and an oscillating fence, and steady and pulsating secondary flow injection at the cavity leading edge.

Presented as Paper 90-4018 at the AIAA 13th Aeroacoustics Conference, Tallahassee, FL, Oct. 22–24, 1990; received June 11, 1991; revision received Oct. 22, 1992; accepted for publication Oct. 28, 1992.

*Engineering Analyst; currently at Veda, Incorporated, Dayton, OH 45431.
†Professor. Associate Fellow AIAA.

Frequency Prediction

From experiments, Rossiter[10] developed a cavity model based on an acoustic feedback mechanism that resembles an acoustic source at the trailing edge.[11] Based on this model, Rossiter proposed a semiempirical relationship for the nondimensional cavity resonant frequency or Strouhal number

$$S = \frac{fL}{U} = \frac{m - \alpha}{M + 1/k} \qquad m = 1, 2, 3, \ldots \tag{1}$$

where m is a positive integer and corresponds to the frequency mode number, α is an empirical constant that takes into account the phase difference between the upstream arrival of the acoustic wave and the subsequent shedding of a vortex, and k is also an empirical constant tied to a disturbance convection speed.[11] Rossiter's values for α and k were $\alpha = 0.25$ and $k = 0.57$. Rossiter's formula assumes that the speed of sound in the cavity is equal to the speed of sound of the freestream. This is equivalent to assuming the cavity temperature recovery factor is equal to zero. Heller et al.[11] determined the actual recovery factor to be more nearly equal to unity. Therefore, the speed of sound in the cavity is equal to the freestream stagnation speed of sound. Consequently, Heller et al.[11] proposed a modification to Rossiter's equation that uses the stagnation speed of sound:

$$S^* = \left(\frac{fL}{U}\right) = \frac{m - \alpha}{\left(M/\{1 + [(\gamma - 1)/2]M^2\}^{1/2}\right) + 1/k}$$

$$m = 1, 2, 3, \ldots \tag{2}$$

The modified equation was used in this study to predict mode frequencies.

Test Apparatus and Procedure

Tests were conducted in a small-scale test section in which the side walls of the cavity also formed the side walls of the flowfield over the cavity. The test section included a two-dimensional nozzle assembly and a flat surface upstream of a rectangular cavity with $L/D = 2$. The cavity dimensions were $L = 2$ in., $D = 1$ in., and $Z = \frac{5}{16}$ in. The leading edge of the cavity was located approximately $2\frac{5}{8}$-in. downstream of the nozzle exit. The nozzle assembly and the cavity were machined from $\frac{5}{16}$-in.-thick aluminum. The entire arrangement was sandwiched between two pieces of 0.75-in.-thick clear Plexiglas®. The sandwiched assembly was bolted to a base plate and mounted on a calming chamber as shown in Fig. 1.

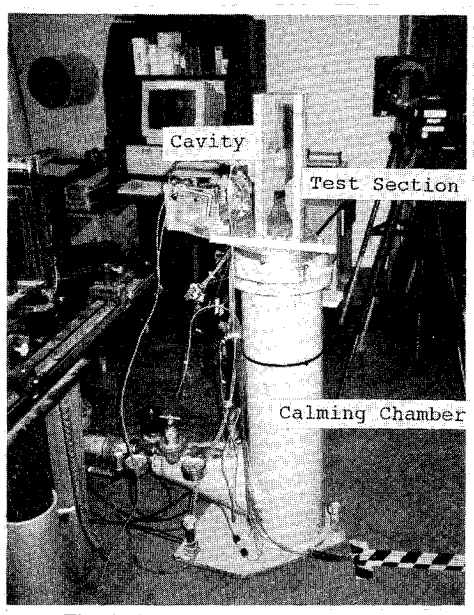

Fig. 1 Photograph of test apparatus.

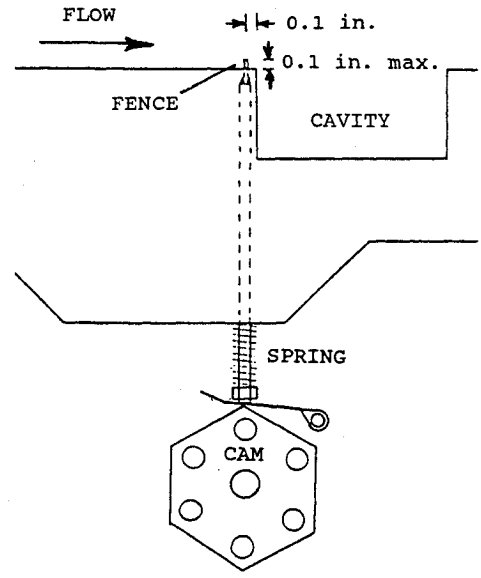

Fig. 2 Fence oscillator mechanism.

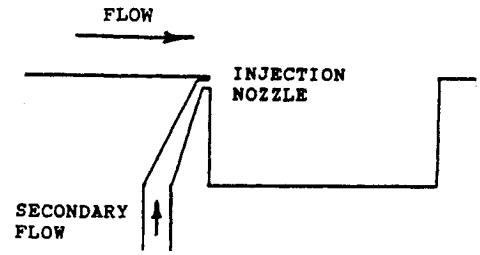

Fig. 3 Parallel flow injection nozzle.

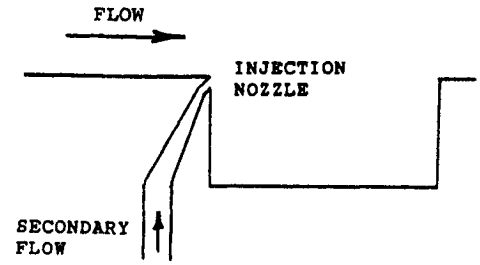

Fig. 4 45-deg flow injection nozzle.

For the fence tests, a variable-height static fence that could also be oscillated was positioned at the leading edge of the cavity. The fence arrangement and the oscillator mechanism are shown in Fig. 2. The fence consisted of a thin metal plate that spanned the $\frac{5}{16}$-in.-wide flow passage. Oscillations were introduced by rotating the cam with a belt and a 24-V dc motor, and were limited to approximately 220 Hz.

Schematics of the secondary flow injection configurations are shown in Figs. 3 and 4. The two designs allowed for flow injection either parallel or 45 deg to the external flow. The exit slot was located 0.02-in. below the surface. The slot height was 0.05 in. and the slot width was $\frac{5}{16}$ in. Steady and pulsating secondary flow was controlled by a ball-type valve and a variable speed motor. Pulsation frequency ranged up to 80 Hz, which was approximately the limit of the pulsator.

Four nozzle assemblies provided six nominal flow Mach numbers upstream of the cavity ($M = 0.6$, 0.7, 0.9, 1.1, 1.3, and 1.5). One nozzle assembly incorporating a smooth converging curve was designed for the three subsonic flow conditions, and three converging-diverging nozzle assemblies were

Table 1 Experimental and calculated parameters

Nozzle Mach number		Cavity Mach number		Mach number used for calculated values of	Calculated nozzle exit velocity		
P_{exit}/P_0	Mass flow rate	Schlieren Mach angle	P_{atm}/P_0	U, Re, and δ	U, ft/s	Calculated Ux/ν, 10^6	Calculated δ, in.
0.58	0.63	N/A	0.58	0.62	677	1.0	0.062
0.73	0.80	N/A	0.74	0.76	816	1.3	0.059
0.87	0.93	N/A	0.89	0.90	947	1.6	0.056
1.03	1.07	1.03	1.07	1.07	1094	2.1	0.053
1.23	1.31	1.28	1.26	1.28	1260	2.7	0.051
1.56	1.53	1.50	1.58	1.53	1432	3.6	0.048

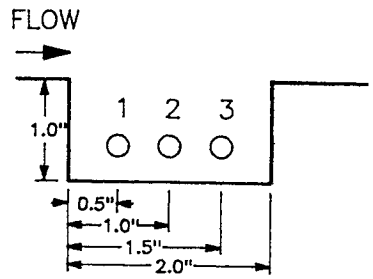

Fig. 5 Pressure transducer locations.

designed for the three supersonic flow conditions. The exit area of each nozzle assembly was identical to allow interchangeability of the nozzles with the surface/cavity assembly. The nozzles were designed to have fully expanded exit flow to ambient pressure at each desired flow condition.

Compressed air was supplied from two compressors, each capable of supplying $\frac{1}{2}$ lbm/s of air at approximately 90 psig. An in-line drier removed moisture and an in-line filter removed particles that could have scratched the Plexiglas. The mass flow rate was measured with an orifice meter, the supply pressure to the calming chamber was regulated with a dome valve, and the nozzle stagnation pressure was measured with a piezoresistive transducer. A second filter was used in the calming chamber to remove any remaining particles in the flow. Static pressures at the nozzle exit and cavity floor were measured with a bank of U-tube mercury manometers.

The clear Plexiglas side panels of the test section allowed for schlieren photography. One side panel was also used to mount the dynamic pressure transducers flush on the side wall of the cavity. Figure 5 shows the location of the transducers in the cavity. While it is more usual to sense pressure on the cavity floor, the transducers were mounted in the side walls for ease of installation. This may lead to variation in measurements compared with other studies. The conditioned and amplified signals were interfaced with a personal computer through an analog-to-digital converter module and stored in data files. All pressure transducers were calibrated statically with a dead weight tester and calibrated dynamically with a precision dynamic calibrator. The pressure transducer data sampling rate was 29,917 Hz. Due to the computer array size limitations, only 2048 data points per channel could be sampled. In addition to recording sound pressure levels, a fourth channel was used to measure either differential pressure across the orifice meter or dynamic pressure amplitude at the entrance of the secondary flow injection nozzle. The discretely sampled pressure data were processed using a fast Fourier transform (FFT) algorithm that provided an output of pressure amplitude (psi) vs discrete frequency (Hz). The pressure amplitude values were then converted to sound pressure level (SPL) in decibels (dB):

$$\text{SPL} = 20 \log_{10} \frac{P_{\text{rms}}}{P_{\text{Re}}} \text{ (dB, } re \text{ 20 } \mu\text{N/m}^2\text{)} \qquad (3)$$

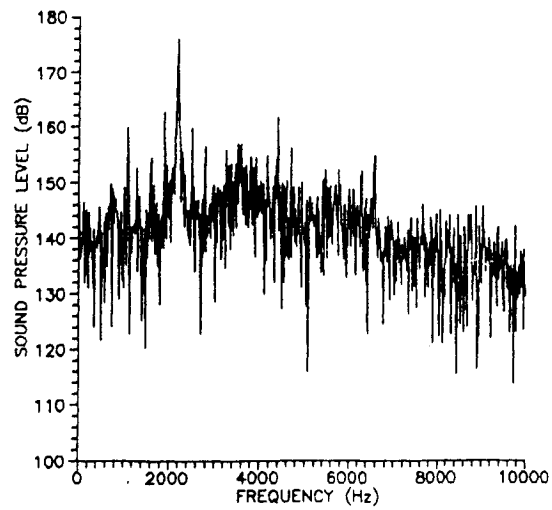

Fig. 6 Baseline SPL spectrum, M = 1.53.

Flow temperature, calming chamber pressure, nozzle exit pressure, and cavity floor static pressure were recorded separately. Schlieren photographs of the flowfield in and above the cavity were taken with a spark duration of approximately $\frac{1}{6}$ μs. This enabled a photograph to show the shear layer, Mach lines, and shock waves.

Results

All SPLs presented are based on measurements from the transducer at location 1 (Fig. 5). In general, the peak SPLs measured at locations 1 and 3 agreed, whereas those at location 2 were equal to those at location 1 or, in some cases, lower by as much as 15 dB. A baseline SPL spectrum (without suppression) was established for each test configuration and flow condition. A typical cavity SPL spectrum (15-Hz bandwidth) for a Mach number of 1.53 without suppression is shown in Fig. 6. The peak cavity SPL occurs at approximately 2200 Hz. This value will be shown later to correspond closely to the mode 1 frequency predicted by Eq. (2).

The flow Mach number for supersonic flow conditions was calculated from the nozzle pressure ratio, the mass flow rate, and from measurements of the angle of a Mach wave on the schlieren photographs. Unsteady behavior, however, in the external flow due to interaction between the external flow and the cavity made it difficult to measure a Mach angle. Schlieren photographs illustrated the unsteadiness, presence of shock waves, and large-scale disturbances in the flow over the cavity. By replacing the cavity with a solid surface, only small disturbances (Mach waves) were present. Consequently, most of the supersonic flow Mach number measurements based on the Mach angle were made without the cavity. For subsonic flow conditions, the mass flow rate obtained from the orifice meter measurements and the nozzle pressure ratio were used to determine the flow Mach number. Calculated and measured Mach numbers are given in Table 1, along with values

of the Mach number selected for calculations and predictions. There was good agreement among the measured and calculated values of the Mach number.

Values of U at the nozzle exit were calculated on the basis of selected values of the flow Mach number and assumed isentropic expansion to the exit pressure. Values of U were then used to calculate the Reynolds number and δ. The boundary-layer thickness at the cavity leading edge was based on turbulent flow, since the lowest Reynolds number at the cavity was higher than the critical Reynolds number for transition. The boundary-layer thickness was estimated from[12,13]

$$\delta = 0.37x(Ux/\nu)^{-1/5} \tag{4}$$

Values of U, Re, and δ are given in Table 1 where Re and δ are based on distance from the nozzle exit. The boundary-layer thickness calculated at the cavity leading edge was approximately 0.05 in. The boundary-layer thickness on the side walls could be as large. Therefore, the boundary layer on the side walls represents a significant portion of the $\frac{5}{16}$-in. depth and undoubtedly affects the flow over the cavity. This is one area that leads to some reservation in using the results.

The modified Rossiter equation for Strouhal number, Eq. (2), was used to predict resonant frequencies within the cavity. Some examples of measured and predicted values of the resonant frequencies are shown in Table 2. The measured values were obtained from baseline SPL spectrums without suppression similar to the spectrum shown in Fig. 6, where mode 1 was predominant. The predicted values compared with the measured values differed by as much as 20%, which is not unusual considering that Heller et al.[11] estimated the difference to be $\pm 10\%$ for cavities with $L/D \geq 4$ and greater for cavities with $L/D < 4$. The predicted mode frequencies, however, are based on the measured Mach numbers, which are subject to measurement errors as well. Furthermore, the frequency identified as mode 2 in Table 2 for $M = 1.53$ appears to be a harmonic of the identified mode 1 rather than an actual mode 2, as predicted by Eq. (2). This is illustrated in the spectrum (Fig. 6), which appears to contain harmonics at 4400 and 6600 Hz of the apparent mode 1 oscillation at 2200 Hz. There were a number of times when an apparent mode 2 oscillation was predominant, such as under some conditions with static and oscillating fences.

Fence Effects

The results in Figs. 7 and 8 are for a static (nonoscillating) fence for different values of fence height (0, 0.02, 0.05, 0.08,

Table 2 Resonant frequency comparison

Mach number	Frequency: Measured, Hz	Frequency: Calculated Eq. (2), Hz	Difference, %
	First mode		
0.62	1600	1296	19
0.76	1700	1483	13
0.90	2000	1648	18
1.07	2177	1812	17
1.28	2147	1981	8
1.53	2191	2131	3
	Second mode[a]		
0.62	3400	3024	−11
0.76	4100	3460	−16
0.90	4200	3845	−8
1.07	4500	4228	−6
1.28	4309	4622	7
1.53	4382	4972	13

[a]Some measured, Hz may be harmonics of the first mode.

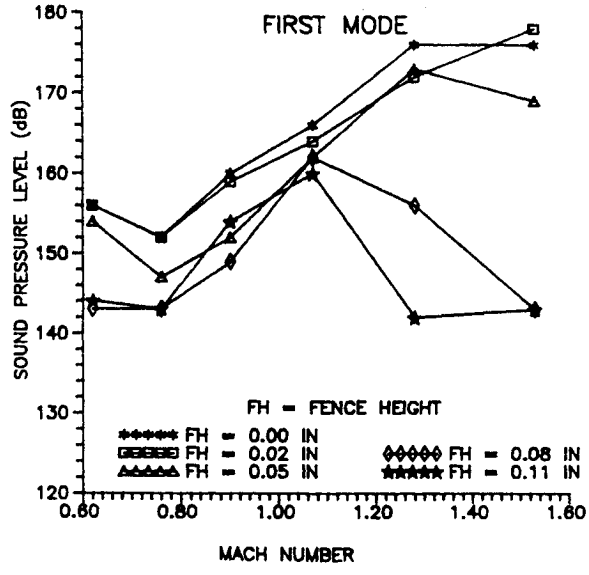

Fig. 7 Effect of fence height and Mach number on cavity SPL (first mode).

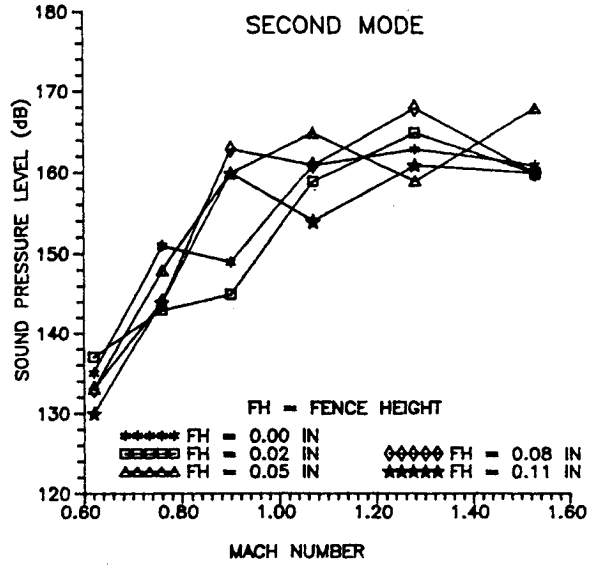

Fig. 8 Effect of fence height and Mach number on cavity SPL (second mode).

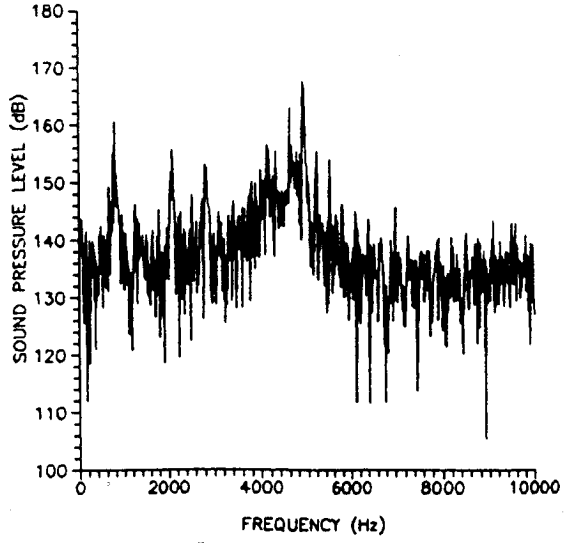

Fig. 9 Pressure spectrum with a $\frac{5}{64}$-in. static fence at $M = 1.28$.

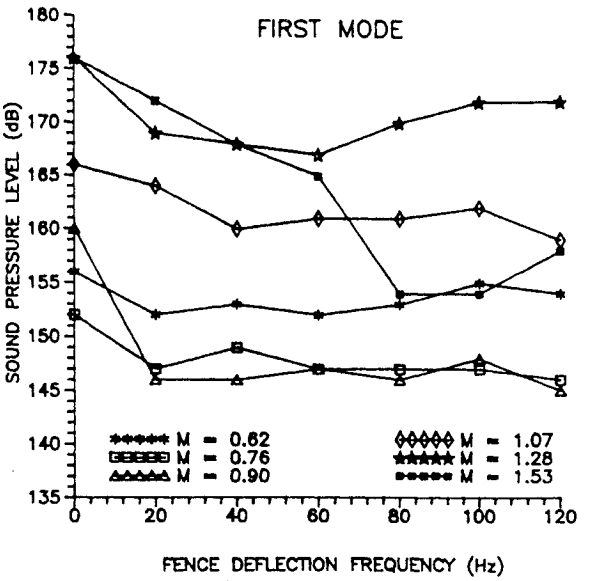

Fig. 10 Effect of fence oscillation on cavity SPL (first mode).

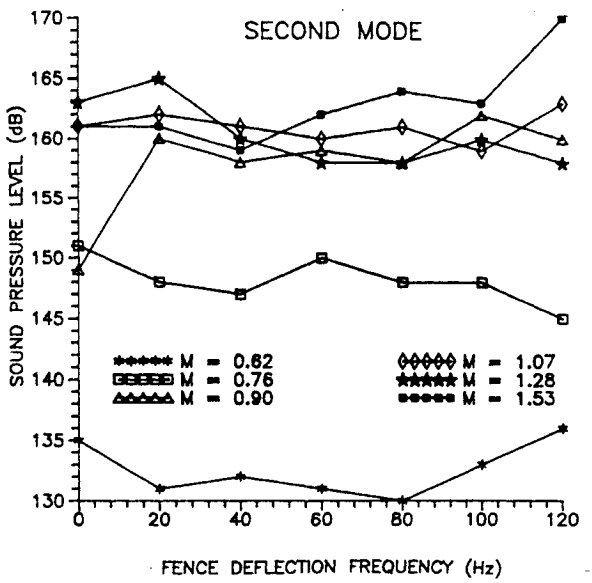

Fig. 11 Effect of fence oscillation on cavity SPL (second mode).

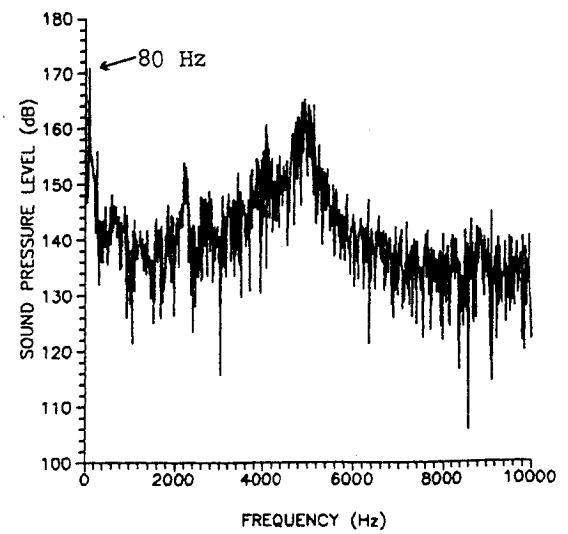

Fig. 12 Pressure spectrum with fence oscillating at 80 Hz, $M = 1.53$.

and 0.11 in.) for the six different values of Mach number. Without fences and with low fence heights (less than the boundary-layer thickness at the cavity leading edge), both mode 1 and mode 2 SPLs tend to increase with increasing Mach number. As shown in Fig. 7, the fence was somewhat effective in reducing the amplitudes of the first mode at the lower Mach numbers, and highly effective at the higher Mach numbers when the fence height exceeded the boundary-layer thickness. The pressure spectrum in Fig. 9 shows that at $M = 1.28$ the reduction in the mode 1 peak amplitude resulted in a predominant mode 2 oscillation at approximately 4800 Hz. This measured frequency is within about 4% of the mode 2 frequency (4622 Hz) predicted by Eq. (2) and shown in Table 2. The second mode was less affected by the fence at all heights tested and at all Mach numbers, except possibly at $M = 0.9$. At this Mach number and at the lower fence heights, the SPL corresponded more closely with that at the lower subsonic Mach numbers, and at the higher fence heights the SPL corresponded more closely with that found at the supersonic Mach numbers.

The effects of the fence when oscillated transversely into the main flow with an amplitude of 0.1 in., over a frequency range from 20 to 120 Hz, are shown in Figs. 10 and 11. The suppression effectiveness of the oscillating fence at these low frequencies was rather limited. Unfortunately, frequencies higher than 220 Hz could not be obtained with the fence oscillator used in this study; however, some data obtained at a single Mach number at frequencies up to 220 Hz showed no significant change in the peak amplitude levels from those obtained at the lower frequencies. The purpose of oscillating the fence was to try to force the shear layer at a frequency different from the cavity/flow resonant frequency. The fence oscillation did force the shear layer and the cavity to respond to the frequency of oscillation. This is clearly evident in the SPL spectrum illustrated in Fig. 12 for a fence oscillation frequency of 80 Hz. The cavity SPL at 80 Hz was about as high as the mode 1 and 2 levels that were to be suppressed. Comparing the results in Fig. 12 with those in Fig. 6 shows that the SPL of mode 1 was reduced considerably, while that of mode 2 was increased and became predominant over mode 1. The mode 2 measured frequency was approximately 5000 Hz, which agrees closely with the predicted value shown in Table 2 for $M = 1.53$.

Effects of Flow Injection

Typical cavity SPLs obtained as a function of steady injection rate from the two flow injection nozzles (45 deg and parallel to the external flow), at $M = 1.28$, are shown in Fig.

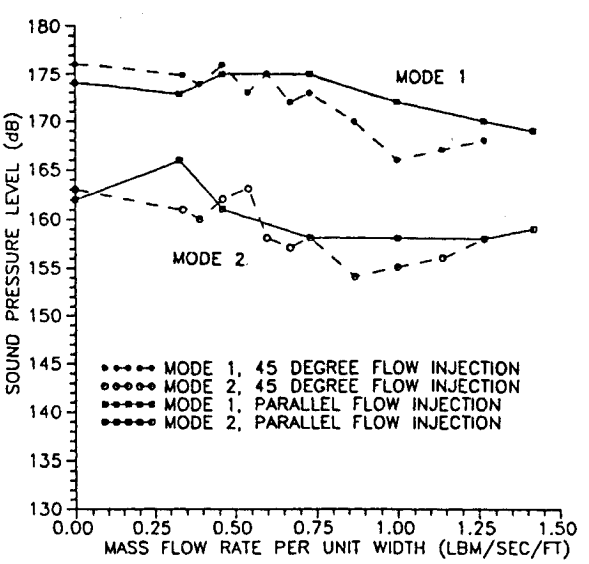

Fig. 13 Effect of flow injection on cavity SPL, $M = 1.28$.

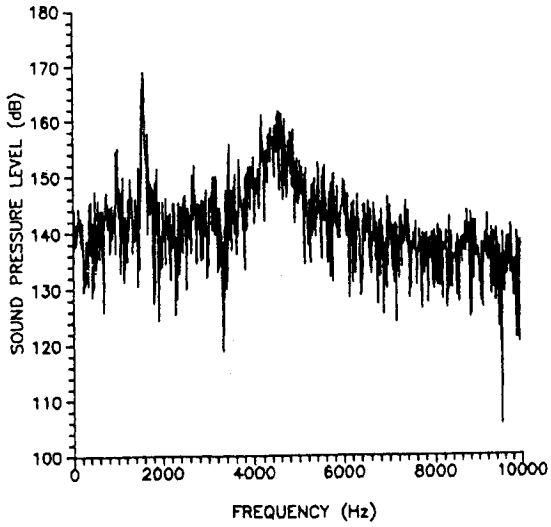

Fig. 14 Pressure spectrum with parallel flow injection and no external flow.

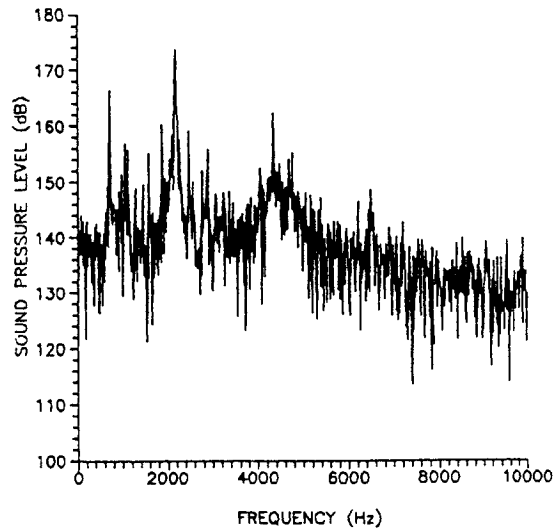

Fig. 15 Pressure spectrum with external flow at $M = 1.28$ and no flow injection.

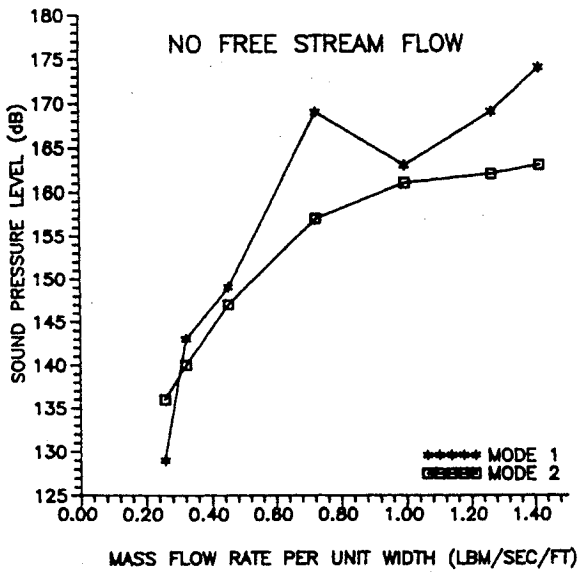

Fig. 16 Effect of parallel flow injection rate on cavity SPL with no external flow.

13. As might be expected, SPL suppression was somewhat better with 45-deg flow injection than with parallel flow injection. In fact, it was found that parallel flow injection alone (without external flow) was able to create disturbances in the cavity (Fig. 14) as large as those found due to external flow. A cavity SPL spectrum with only external flow at $M = 1.28$ is shown in Fig. 15 for comparison with Fig. 14. The effects of flow injection rate on the cavity SPL without external flow are shown in Fig. 16 for the first two modes. There was a substantial increase in the SPL with an increase in flow injection rate, which may explain why flow injection parallel to the external flow was not as effective as other means for suppressing large amplitude cavity pressure oscillations. It also suggests that the cavity can be excited by the shear layer.

Pulsating flow injection had little effect beyond that of steady flow injection in suppressing cavity pressure oscillations, but the pulsation amplitude decreased as the frequency increased. Without pulsations, the 10, 30, and 50 psig supply pressures correspond to injection mass flow rates of approximately 0.3, 0.6, and 0.9 lbm/s/ft, respectively. With pulsations, however, the flow rate decreased as frequency increased for a given supply pressure. Figure 17 shows only a slight effect of a

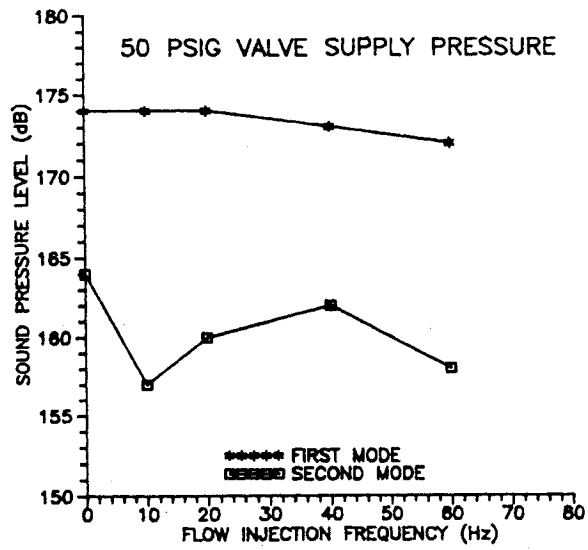

Fig. 17 Effect of pulsating parallel flow injection on cavity SPL, $M = 1.28$.

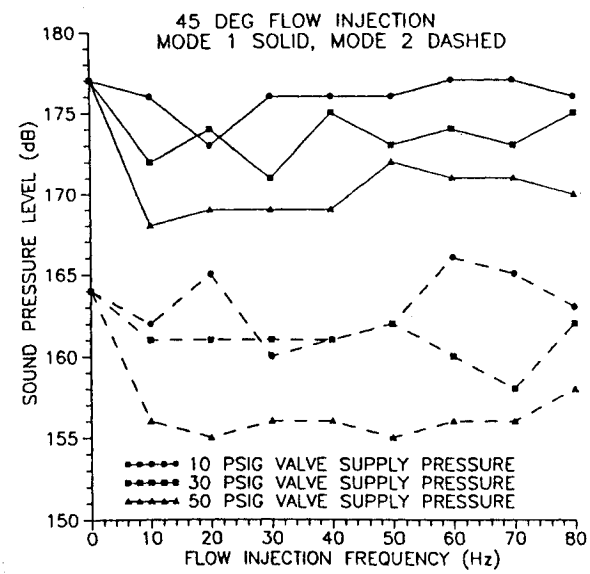

Fig. 18 Effect of pulsating 45-deg flow injection on cavity SPL, $M = 1.28$.

parallel injection pulsating flow on the cavity SPL at $M = 1.28$. Pulsating 45-deg flow injection is shown in Fig. 18. Some reduction in SPL is shown at the highest supply pressure over most of the frequency range.

Conclusions

Methods for suppressing flow-induced pressure oscillations in shallow cavities due to subsonic and supersonic flows over the cavity were examined. Tests were conducted in a small-scale apparatus in which the side walls of the cavity also formed the side walls of the flowfield over the cavity. Boundary-layer buildup on the side walls of the flowfield could affect the results. Measured cavity resonant and first and second mode frequencies were within 20% of predicted values based on measured Mach number. Unsuppressed SPLs generally increased with Mach number, and were as high as 175 dB at flow Mach numbers of 1.28 and 1.53 (highest tested). A static fence at the leading edge of the cavity was the most effective of the suppression methods considered. At Mach numbers of 1.28 and 1.53, the first mode SPLs decreased as much as 30 dB when the fence height was about equal to or greater than the boundary-layer thickness at the cavity leading edge. The second mode SPLs were not affected by the fence nearly as much. An oscillating fence at 80 Hz did reduce the first mode SPL, but generally caused as high or higher SPL at the oscillation frequency. Steady flow injection at a 45-deg angle to the flow at the cavity leading edge was somewhat more effective in reducing SPL (as much as 10 dB) than parallel flow injection. Steady parallel flow injection at the cavity leading edge without an external flow tended to excite the cavity similar to that of an external flow. The SPL increased with increase in injection mass flow rate up to a SPL of almost 175 dB. Pulsating 45-deg flow injection reduced the SPL about the same as that found with steady flow injection at the same flow rate. Pulsating parallel flow injection was not as effective for suppression as pulsating 45-deg flow injection.

References

[1]Komerath, N. M., Ahuja, K. K., and Chambers, F. W., "Prediction and Measurement of Flows over Cavities—A Survey," AIAA Paper 87-0166, Jan. 1987

[2]Rockwell, D., "Oscillation of Impinging Shear Layers," *AIAA Journal*, Vol. 21, No. 5, 1983, pp. 645–664.

[3]Rockwell, D., and Naudascher, E., "Review—Self-Sustaining Oscillations of Flow Past Cavities," *Journal of Fluids Engineering*, Vol. 100, June 1978, pp. 152–165.

[4]Karamcheti, K., "Acoustic Radiation from Two-Dimensional Rectangular Cutouts in Aerodynamic Surfaces," NACA TN 3487, Aug. 1955.

[5]Heller, H. H., and Bliss, D. B., "Aerodynamically Induced Pressure Oscillations in Cavities—Physical Mechanisms and Suppression Concepts," Air Force Flight Dynamics Lab. TR-74-133, Wright-Patterson AFB, OH, 1975.

[6]Heller, H. H., and Bliss, D. B., "The Physical Mechanism of Flow-Induced Pressure Fluctuations in Cavities and Concepts for Their Suppression," AIAA Paper 75-491, March 1975.

[7]Franke, M. E., and Carr, D. L., "Effect of Geometry on Open Cavity Flow-Induced Pressure Oscillations," *Aeroacoustics: STOL Noise; Airframe and Airfoil Noise*, Vol. 45, Progress in Astronautics and Aeronautics, AIAA, New York, 1976, pp. 297–314.

[8]Sarohia, V., and Massier, P. F., "Control of Cavity Noise," *Journal of Aircraft*, Vol. 14, No. 9, 1977, pp. 833–837.

[9]Covert, E. E., "An Approximate Calculation of the Onset Velocity of Cavity Oscillations," *AIAA Journal*, Vol. 8, No. 12, 1970, pp. 2189–2194.

[10]Rossiter, J. E., "Wind Tunnel Experiments on the Flow over Rectangular Cavities at Subsonic and Transonic Speeds," Royal Aircraft Establishment, Aeronautical Research Council, R&M 3438, 1966.

[11]Heller, H. H., Holmes, D. G., and Covert, E. E., "Flow Induced Pressure Oscillations in Shallow Cavities," *Journal of Sound and Vibration*, Vol. 18, No. 4, 1971, pp. 545–553.

[12]Charwat, A. F., Roos, J. N., Dewey, F. C., Jr., and Hitz, J. A., "An Investigation of Separated Flows—Part I: The Pressure Field," *Journal of the Aerospace Sciences*, Vol. 28, No. 6, 1961, pp. 457–470.

[13]Schlichting, H., *Boundary Layer Theory*, 4th ed., McGraw-Hill, New York, 1960.